



# Microbial fuel cell: Interplay of energy production, wastewater treatment, toxicity assessment with hydraulic retention time

Ana Carla Sorgato<sup>a,\*</sup>, Thamires Custódio Jeremias<sup>a</sup>, Fernanda Leite Lobo<sup>b</sup>, Flávio Rubens Lapolli<sup>a</sup>

<sup>a</sup> Department of Sanitary and Environmental Engineering, Federal University of Santa Catarina (UFSC), Campus Universitário, Trindade, 88.040-900, Florianópolis, SC, Brazil

<sup>b</sup> Department of Hydraulic and Environmental Engineering, Federal University of Ceará (UFC), Campus Do Pici, 60.440-900, Fortaleza, CE, Brazil

## ARTICLE INFO

### Keywords:

Microbial fuel cell  
Upscaling  
Domestic wastewater treatment  
Power generation  
Phytotoxicity

## ABSTRACT

Microbial fuel cell (MFC) operation under similar conditions to conventional methods will support the use of this technology in large-scale wastewater treatment. The operation of scaled-up air-cathode MFC (2 L) fed with synthetic wastewater (similar to domestic) in a continuous flow was evaluated using three different hydraulic retention times (HRT), 12, 8, and 4 h. We found that electricity generation and wastewater treatment could be enhanced under an HRT of 12 h. Additionally, the longer HRT led to greater coulombic efficiency (5.44%) than MFC operating under 8 h and 4 h, 2.23 and 1.12%, respectively. However, due to the anaerobic condition, the MFC was unable to remove nutrients. Furthermore, an acute toxicity test with *Lactuca sativa* revealed that MFC could reduce wastewater toxicity. These outcomes demonstrated that scaled-up MFC could be operated as a primary effluent treatment and transform a wastewater treatment plant (WWTP) into a renewable energy producer.

## 1. Introduction

Effective wastewater management is a crucial challenge in modern-day society due to the substantial energy requirements and costly treatment procedures. According to Li et al. (2015), the global electricity consumption for wastewater treatment could reach up to 3%. This highlights the urgent need to reduce energy consumption in wastewater treatment as a means of mitigating the impact of climate change (Colares et al., 2021). To address this issue, novel technologies that can provide efficient wastewater treatment solutions are crucial (Rossi and Logan, 2022). One such technology is the microbial fuel cell (MFC).

MFCs are bio-electrochemical reactors capable of producing power from wastewater without any external energy source during wastewater treatment (Dwivedi et al., 2022). MFC can be described as a battery operated by electroactive bacteria (EAB), which develop a biofilm at the anode, and degrade the organic matter present in wastewater (Logan et al., 2019). During this process, the electrons generated by EAB are transferred to the anode and flow through an external copper wire with an external resistor to the cathode (Munoz-Cupa et al., 2021). At the cathode, the electrons and protons (H<sup>+</sup>) are used in the oxygen reduction

reaction (ORR) to produce electrical power (Rossi et al., 2018). MFCs offer unique advantages over conventional biotreatment processes, including direct electricity generation, low sludge yield, and low carbon footprint (Luo et al., 2023).

Despite their advantages, scaling up MFCs and operating them under conditions similar to those found in domestic wastewater treatment plants remain a challenge, due to internal resistance, hydrodynamics, electrode life-span, cost and production, and dissolved oxygen diffusion (Rossi and Logan, 2022). In order to demonstrate sufficient MFC performance to provide a path forward for implementation of this technology under domestic WWTPs, there have been many studies addressing the scaling-up and the optimal conditions, mainly the hydraulic retention times (HRT) under continuous operation (Deng et al., 2023; Yu et al., 2021).

The HRT has a remarkable effect on electricity production and wastewater treatment. Sugioka et al. (2022) operated an air-cathode MFC with 226 L, ranging the HRT from 9 to 42 h, achieving 0.072–0.51 W m<sup>-3</sup> of power density and 31–58% for COD (chemical oxygen demand) removal. Hiegemann et al. (2019) demonstrated the operation of a 255 L single chamber MFC, ranging the HRT from 43 to

\* Corresponding author.

E-mail addresses: [ana.sorgato@gmail.com](mailto:ana.sorgato@gmail.com), [ana.sorgato@posgrad.ufsc.br](mailto:ana.sorgato@posgrad.ufsc.br) (A.C. Sorgato).

<https://doi.org/10.1016/j.envres.2023.116159>

Received 30 January 2023; Received in revised form 8 May 2023; Accepted 14 May 2023

Available online 20 May 2023

0013-9351/© 2023 Elsevier Inc. All rights reserved.

12 h. The obtained results demonstrated a maximal power density of  $0.32 \text{ W m}^{-3}$  and COD removal efficiency of 41%, under the highest HRT. Then, finding the required optimal HRT is imperative to design an effective system (Bird et al., 2022).

Furthermore, wastewater quality monitoring plays an important role in MFC technology. However, the chemical analyses applied to monitor water quality can only measure some pollutants, such as COD, nitrogen, and phosphorous, which are not always in accordance with toxic effects of wastewater (Yu et al., 2019). On the other hand, toxicity tests can detect the mixture effects of all chemicals in a sample and provide adverse biological effects (Lutterbeck et al., 2020). To demonstrate adequate MFC performance for implementation, it is important to verify the possible toxic effects of effluent generated by MFC. Previous studies have observed a decrease in toxicity levels of MFC effluent from wetland-MFC treating laundry hospital wastewater using the micro-crustacean *Daphnia magna* and lettuce (*Lactuca sativa*) seeds (Lutterbeck et al., 2020) and dairy wastewater treated by air-cathode MFC also using microcrustacean (*Daphnia similis*) (Marassi et al., 2020a). Nevertheless, there is a knowledge gap on the effluent toxicity produced by MFCs treating municipal wastewater.

Therefore, the aim of this study is to address the optimal operational condition of an air-cathode MFC with a working volume of 2 L MFC for domestic wastewater treatment. The performance and efficiency were evaluated under continuous flow mode and different HRT similar to those applied in conventional wastewater treatment methods. The power generation and pollutant removal efficiencies were determined for each tested HRT. In addition, the toxicity of the raw wastewater and MFC effluent generated was determined by exposure to the *L. sativa* seeds.

## 2. Materials and methods

### 2.1. MFC construction

The MFC used in this study were single-chamber, air-cathode and were fabricated using acryl sheets with an anodic work volume of 2 L. Air cathode was composed of a membrane electrode assembly (MEA), with a nominal area of  $132 \text{ cm}^2$ . The MEA was made up of a Nafion™ (212) membrane, which operated as a separator and carbon based materials as electrodes. The membrane was sandwiched between a carbon paper anode (gas diffusion layer - GDL) and cathode (gas diffusion electrode - GDE) coated with a catalyst concentration of  $0.4 \text{ mgPt cm}^{-2}$  (Novo-cell, Americana, Brazil). The MEA also contain carbon nanoparticle (Vulcan XC 72 R), which provides excellent electron conductivity, and polytetrafluoroethylene (PTFE) layer, to avoid the oxygen diffusion into the anode and water leak in the air-cathode. The MEA were placed at the cathode site of the cells. Stainless steel plates were used as electron collectors. The electrode and current collector were sandwiched between two gaskets frames to seal the chamber. A single copper wire connected the electrodes externally with an external resistor.

### 2.2. MFC operation

The inoculum source was sludge taken from an anaerobic tank installed at a municipal wastewater treatment plant (Florianópolis, Brazil). So, the MFC was inoculated with anaerobic sludge (50 mL) and a growth medium (Lobo et al., 2017). The procedure was previously reported by Sorgato et al. (2022). After 15 days, the MFC reached a stable operation, and the growth medium was replaced by synthetic wastewater similar to domestic wastewater as the substrate. After that, the MFC was applied to treat wastewater at different HRT (12, 8, and 4 h) with a fixed influent COD concentration. As the HRT was reduced, the organic load rate (OLR) increased, with the OLR ranging between 1 and  $2.94 \text{ kgCOD m}^{-3} \text{ d}^{-1}$ . The values are comparable to those applied for high-rate domestic wastewater treatment systems, such as activated

sludge  $<3 \text{ kgCOD m}^{-3} \text{ d}^{-1}$  (Metcalf, 2014).

Three distinct periods, each lasting 15 days, were used to assess the MFC performance (Table 1). During the operation, the temperature was kept in  $30 \text{ }^\circ\text{C}$ , influent pH of 7.5 and external resistance ( $R_{\text{ext}}$ ) of  $1000 \text{ } \Omega$ . The MFC was fed in a continuous mode using a peristaltic pump (Watson Marlow, 323-S). The MFC setup could be seen in Fig. 1.

The synthetic wastewater, with similar characteristics to municipal one, was prepared according to the following composition (Souza et al., 2020):  $850 \text{ mg L}^{-1}$  of  $\text{CH}_3\text{COONa}$ ,  $170 \text{ mg L}^{-1}$  of  $\text{KH}_2\text{PO}_4$ ,  $280 \text{ mg L}^{-1}$  of  $\text{NH}_4\text{Cl}$ ,  $10 \text{ mg L}^{-1}$  of  $\text{MgSO}_4 \cdot 7\text{H}_2\text{O}$ ,  $7.3 \text{ mg L}^{-1}$  of  $\text{CaCl}_2 \cdot 2\text{H}_2\text{O}$ ,  $0.2 \text{ mg L}^{-1}$  of  $\text{CuSO}_4 \cdot 5\text{H}_2\text{O}$ ,  $2.2 \text{ mg L}^{-1}$  of  $\text{ZnSO}_4 \cdot 7\text{H}_2\text{O}$ ,  $0.5 \text{ mg L}^{-1}$  of  $\text{CoCl}_2 \cdot 6\text{H}_2\text{O}$ ,  $5.00 \text{ mg L}^{-1}$  of  $\text{FeSO}_4 \cdot \text{H}_2\text{O}$ , and  $2.15 \text{ mg L}^{-1}$  of  $\text{NaCl}$ .

### 2.3. Data analysis

The influent and effluent samples from were analyzed twice a week, in duplicate. The concentrations of COD, ammoniacal nitrogen ( $\text{NH}_4^+$ ), orthophosphate ( $\text{PO}_4^{3-}$ ), and total nitrogen (TN) were measured by spectrophotometry (Hach DR5000). The  $\text{PO}_4^{3-}$  concentration was determined using the molybdovanophosphoric acid method (APHA, 2005). The concentration of  $\text{NH}_4^+$  was measured via Nessler's Reagent spectrophotometry (APHA, 2005). COD and TN were determined using the Hach 8000 and 10072 methods, respectively, following the manufacturer's instructions. Total suspended solids (SS) was determined by gravimetric method. Total alkalinity was measured by the titrimetric method. The cation and anion ( $\text{CH}_3\text{COO}^-$ ,  $\text{Cl}^-$ ,  $\text{NO}_3^-$ , and  $\text{SO}_4^{2-}$ ) concentrations were assessed by ion chromatography (DIONEX ICS-5000). pH, conductivity, dissolved oxygen (DO) and temperature were obtained using a multiparametric probe (AKSO, AK88).

The voltages were measured every 3 min using a digital multimeter (ET-2615 A, Minipa). Once the voltage was recorded, the current,  $I$  (mA), was calculated according to Ohmic law, where  $E$  is the voltage (mV) and  $R_{\text{ext}}$  is the external resistance ( $\Omega$ ) (Eq. (1)), and power,  $P$  (mW), was calculated according to Eq. (2) (Logan et al., 2006). Current density and power density were determined using the area of the electrode and MFC volume.

$$I = \frac{E}{R_{\text{ext}}} \quad (1)$$

$$P = I \times E \quad (2)$$

Coulombic efficiency (CE, %), defined as the fractional recovery of electrons from the substrate, was calculated according to Eq. (3), where  $M$  is the molecular weight of oxygen ( $32 \text{ g mol}^{-1}$ ),  $I$  is the average current (mA),  $F$  is Faraday's constant ( $96,485 \text{ C mol}^{-1}$ ),  $n$  is the number of electrons ( $4 \text{ mol e}^- \text{ mol O}_2^{-1}$ ),  $q$  is the volumetric influent flow rate ( $\text{L s}^{-1}$ );  $\Delta\text{COD}$  is the change in COD over time ( $\text{mg L}^{-1}$ ) (Logan et al., 2006).

$$\text{CE} = \frac{M \cdot I}{F \cdot n \cdot q \cdot \Delta\text{COD}} \quad (3)$$

The polarization curves were obtained by setting the MFC to open circuit condition for at least 30 min and lowering the external resistance every 10 min, from 1000 to  $10 \text{ } \Omega$  (Yang et al., 2020). The voltage was read by a digital multimeter. The volumetric power density was

**Table 1**  
Operational strategies.

| Parameters                                   | Strategies |       |       |
|--|------------|-------|-------|
|  | I          | II    | III   |
| Period (days)                                | 1–15       | 15–30 | 30–45 |
| HRT (day)                                    | 0.5        | 0.33  | 0.17  |
| Flow rate ( $\text{L day}^{-1}$ )            | 4          | 6.06  | 11.76 |
| Influent COD ( $\text{mg L}^{-1}$ )          | 650        | 650   | 650   |
| OLR ( $\text{kgCOD m}^{-3} \text{ d}^{-1}$ ) | 1.00       | 1.51  | 2.94  |

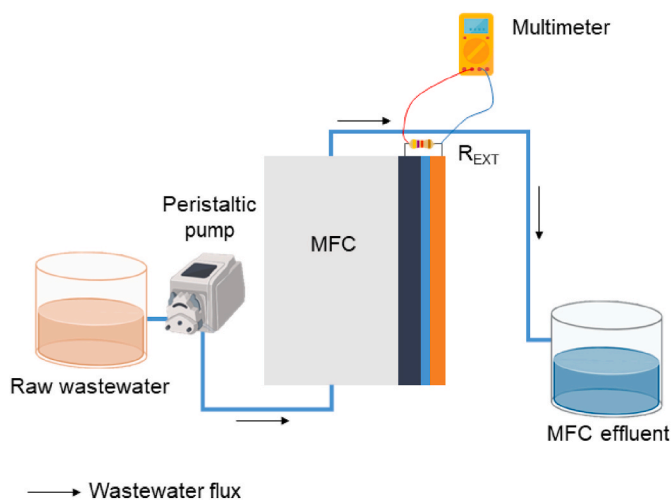


Fig. 1. MFC setup.

normalized to the anodic volume and electrode area.

#### 2.4. Phytotoxicity assay

*Lactuca sativa* seeds were used to evaluate the phytotoxicity of the effluents following the methodology proposed by Sobrero and Ronco (2004). The *L. sativa* seeds utilized in this study were of the same variety and lot (*L. sativa* curly variation, ISLA PRO), with no chemical treatment. The test involves exposing the seeds for 120 h at 22 °C without any light in Petri dishes with a diameter of 100 mm and a filter paper (Jeremias, 2019). The filter paper was soaked in 2 mL of raw wastewater and MFC effluent samples (100, 75, 50, 25%, and 0%) prior to seed exposure. The negative control was mineral water. Ten seeds were exposed in each dish for each test, which was carried out in triplicate, resulting in a total of 120 seeds (Lutterbeck et al., 2020).

The quantity of *L. sativa* seeds that germinated and the lengths of their epicotyl and roots were measured for each sample in order to assess the phytotoxicity. The germination index (GI) was determined by Eq. (4) (Gerber et al., 2017). The percentage of seeds that germinate in sample dishes divided by the total number of seeds that germinate in control dishes is known as seed germination (SG). Root length (RL) is calculated by dividing the percentage of root length of seeds in sample plates by the root length of seeds in control dishes.

$$GI(\%) = \frac{SG \cdot RL}{100} \quad (4)$$

#### 2.5. Statistical analysis

The Shapiro-Wilk test was used to assess the normality of the data. ANOVA was employed to analyze the differences between means from data which had a normal distribution, followed by the Tukey test. The medians for the non-normally distributed data were examined using the non-parametric Kruskal-Wallis and Dunn tests. A comparison of the correlation between operating and physical variables was done using Pearson's correlation (parametric data) and Spearman's correlation (non-parametric data) (Cano et al., 2021). The findings of the *L. sativa* experiments were evaluated using one-way ANOVA, followed by Dunnett's multiple comparison test at a significance level of 0.05. The effluent concentrations reducing lettuce growth in 50% (half maximal effective concentration - EC<sub>50</sub>) were estimated via non-linear regression models, according to Environmental Canada (2007). The Statistica® 13 software was used to conduct these statistical analyses.

### 3. Results and discussion

#### 3.1. Electricity generation

The effects of HRT on power output in the MFC reactor were investigated during time periods of 12, 8, and 4 h. The COD influent concentration was kept at 640 mg L<sup>-1</sup>. The OLR range from 1.00 to 2.94 kgCOD m<sup>-3</sup> d<sup>-1</sup>. These selected values were accordingly to conventional wastewater treatment (Metcalf, 2014).

Fig. 2 depicts the variations in maximal current density at different HRTs. The obtained values showed a statistically significant difference ( $p < 0.05$ ). The current density gradually decreased with the reduction of HRT. The average current density was 159.20, 119.57, and 97.18 mA m<sup>-3</sup> with changing the HRT from 12 to 4 h. There was a significant correlation between the HRT and current density ( $R^2 = 0.7932$ ). The results of the correlational analysis confirm that higher HRT cause an increase in electricity generation. Table 2 shows the other electrochemical results.

The power density also decreased with HRT changing. The higher value was obtained at HRT of 12 h ( $52.04 \pm 18.00$  mW m<sup>-3</sup>). Strategies II and III produced  $29.31 \pm 9.80$  and  $18.98 \pm 2.87$  mW m<sup>-3</sup>, respectively. Similar behavior was found by Sharma and Li (2010), who ranged the HRT from 6.5 to 50 h. They observed that the power density reached 3872 mW m<sup>-3</sup> at 6.5 h and gradually increased to 4072 mW m<sup>-3</sup> at 13.1 h. After that, the power density decreased to 3136 mW m<sup>-3</sup> (50 h). Liu et al. (2008) also demonstrated that the power density increased with higher HRT. At 4.1 h, the MFC produced 17 W m<sup>-3</sup>. When the HRT was extended to 11.3 h and 16 h, the power density increased to 22 and 20 W m<sup>-3</sup>, respectively. A possible explanation for this might be that low HRT does not provide enough time to degrade the substrate until a concentration can no longer convert it into current (Bird et al., 2022).

The observed drop in power density as the HRT decreased could also be attributed to the high flux conditions accompanying low HRT. This reduction in power generation may be due to unfavorable mixture conditions. In support of this, Sobieszuk et al. (2017) demonstrated through mathematical modeling that elevated fluxes (i.e., lower HRT) can result in worse mixture conditions and drop the energy production.

In addition to affecting current density and power density, HRT variations also have a direct influence on the type and amount of bacteria present in the reactor and anode biofilm (Sharma and Li, 2010; Sobieszuk et al., 2017; Walter et al., 2022). High flux increase in cell washout, which can affect the performance of the MFC. Pentead et al. (2016) observed that as HRT decreases and sludge age decreases, the growth rate of microorganisms in the MFC must increase in order to avoid washout.

Moreover, Haavisto et al. (2017) pointed out that at the lowest HRT, current densities and cell voltages decreased due to the increase in the volatile fatty acids concentrations. This suggests that the biofilm could

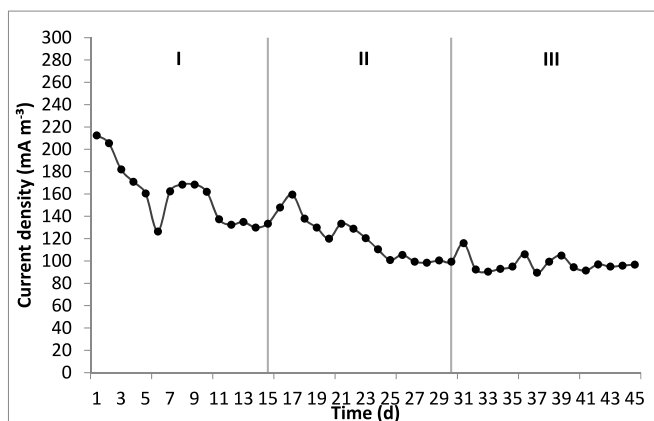


Fig. 2. Current density at different HRT.

**Table 2**

Mean values and standard deviations of current density, electrical power and electrical energy for each phase.

| HRT (h) | OLR (kg m <sup>-3</sup> d <sup>-1</sup> ) | Voltage (V) | Current density       |                       | Power density         |                       |
|---------|---|-------------|-----------------------|-----------------------|-----------------------|-----------------------|
|         |   |             | (mA m <sup>-2</sup> ) | (mA m <sup>-3</sup> ) | (mW m <sup>-2</sup> ) | (mW m <sup>-3</sup> ) |
| 12      | 1.00                                      | 0.32 ± 0.05 | 24.08 ± 4.08          | 159.20 ± 26.30        | 7.87 ± 2.72           | 52.04 ± 18.00         |
| 8       | 1.51                                      | 0.24 ± 0.04 | 18.08 ± 2.96          | 119.57 ± 19.59        | 4.43 ± 1.48           | 29.31 ± 9.80          |
| 4       | 2.94                                      | 0.19 ± 0.01 | 14.70 ± 1.06          | 97.18 ± 7.03          | 2.87 ± 0.43           | 18.98 ± 2.87          |

utilize those substances as an electron acceptor rather than the anode.

Ye et al. (2020) reported an opposing finding, stating that increasing HRT may negatively affect the voltage generation in MFCs. The authors suggested that high HRT could lead to lower substrate concentrations and reduced cell metabolism at the anode chamber, inhibiting the MFC reactor from producing energy. As Zhao et al. (2022) observed, longer HRTs result in greater energy losses. The variation in previous study findings may be attributed to differences in the MFC configuration, electrode material, substrate, biofilm, and other factors (Fadzli et al., 2021).

At the end of each strategy, a polarization curve was obtained by decreasing the external resistance from 1000 to 10 Ω. According to Breheny et al. (2019), the maximal power density is obtained when the external and internal resistance are equal ( $R_{int} = R_{ext}$ ). Therefore, when

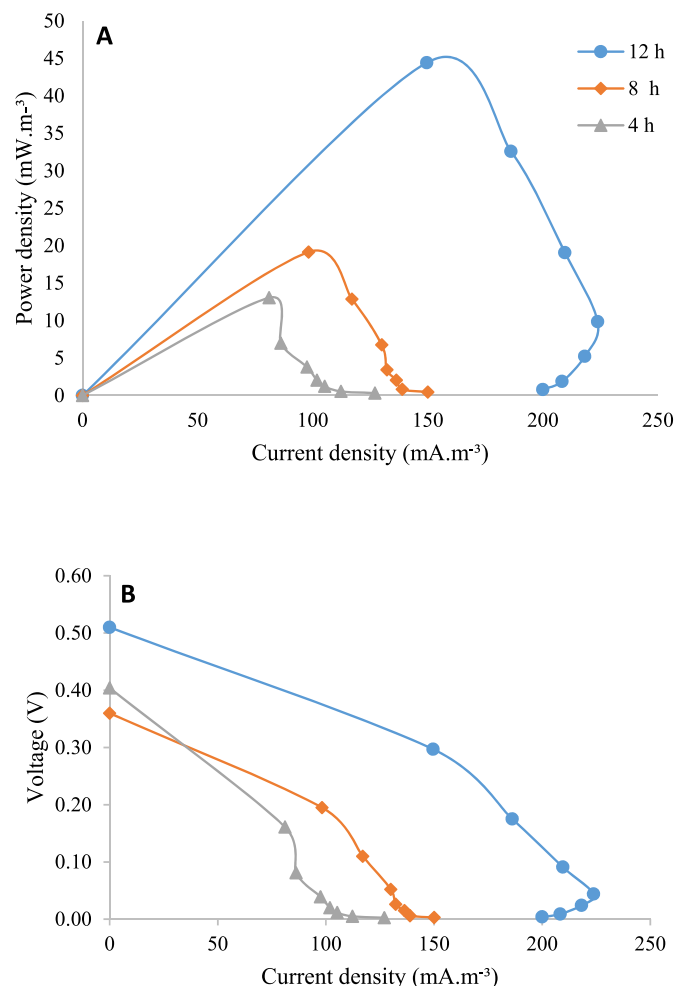


**Fig. 3.** Power (A) and polarization (B) curve.

these values are different, electricity generation losses occur. As shown in Fig. 3, the maximal power density was 44.42 mW m<sup>-3</sup> at an HRT of 12 h, which was 2.32 and 3.40 times higher than the results obtained in HRT of 8 and 4 h, respectively.

A decrease in power density was observed with increasing OLR, which is consistent with the observed trends in voltage, current and power values (Table 2). Subha et al. (2019) and Tamilarasan et al. (2017) also found that maximum power density dropped while the HRT was decreased.

One reason for this can be that higher OLR may be able to outperform the capacity of electroactive bacteria for oxidation and allow other microbial populations in the anode chamber to use the available substrate (Subha et al., 2019). A high loading rate induces ohmic, kinetic, and transport losses. For instance, under higher influent flow rates, could happen insufficient substrate transfer to biofilm and proton transfer into the cathode chamber, which indicates mass transfer and diffusion limitations (Haavisto et al., 2017). Therefore, higher internal resistances produce lower power densities (Opoku et al., 2022). In addition, this power density drop under higher OLR could be attributed to a lack of sufficient contact time for the microbial activity to reach saturation and for the degradation of organic substances, which impair the MFC's ability to produce power (Tamilarasan et al., 2017).

Although it is challenging to make accurate comparisons, the best outcomes have been obtained when employing small volumes and low to medium-strength loads (Marassi et al., 2020a). There is probably an ideal HRT for the electricity generation of each continuously operated MFC reactor, even though these optimum values differ amongst MFC setups (Sobieszuk et al., 2017; Ye et al., 2020). In this study, optimizing HRT to generate electricity in the air-cathode MFC operating in a continuous flow mode was one of the main objectives. For this reason, the HRT of 12 h could satisfy this purpose. It is worth noting that the optimal conditions for one type of MFC are not necessarily the same to another type.

### 3.2. Wastewater treatment performance

The performance of an air-cathode MFC, operated under continuous flow conditions and applied to domestic wastewater treatment, was evaluated based on its removal efficiency for COD, nitrogen, and phosphorus compounds.

#### 3.2.1. COD removal efficiency

The efficiency of the MFC in removing COD was evaluated under three different HRT scenarios, as illustrated in Fig. 4. The average COD removal efficiencies were 20.0%, 21.0%, and 16.3% for HRTs of 12, 8, and 4 h, respectively.

The beginning of each strategy produced stress on microorganisms due to the changes in flow velocity and operational conditions. After the

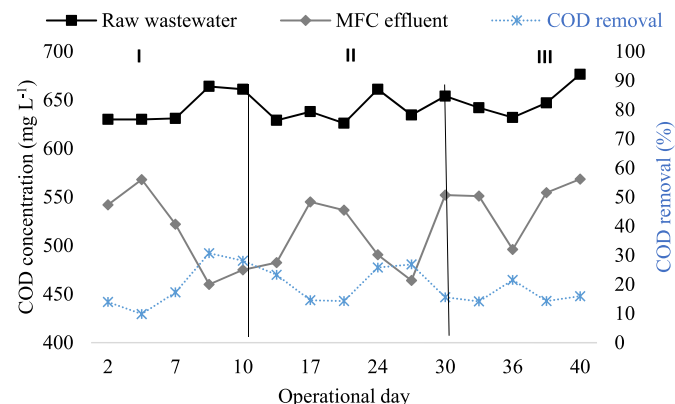


**Fig. 4.** Average removal of COD at different HRTs (18, 8 and 4 h).

MFC achieved the stabilization under each strategy, the COD removal efficiency in strategy I was  $29.43 \pm 1.82\%$ , which was significantly different ( $p < 0.05$ ) from strategy II ( $26.33 \pm 0.76\%$ ) and III ( $15.13 \pm 1.18\%$ ). Moreover, the strategy I achieved the highest COD removal efficiency (30.72%), while strategies II and III, the maximum COD removal was 26.87% and 21.52%, respectively. These results suggest that higher HRT favors COD removal efficiency ( $R^2 = 0.9295$ ).

Sugioka et al. (2022) observed the same behavior during the treatment of municipal wastewater using MFC. The COD removal was  $31 \pm 8.3\%$  at an HRT of 9 h, gradually increased to  $57 \pm 10\%$  at an HRT of 24 h, and increased to  $57 \pm 10\%$  under 42 h. A similar trend was also observed by Kim et al. (2015), which found COD removal equal to  $64.8 \pm 1.7\%$  at an HRT of 8.8 h, decreasing to  $32.8 \pm 1.9\%$  at 2.2 h. Ahn and Logan (2010) also found similar results when operating an air-cathode MFC with domestic wastewater in a continuous flow at an OLR of  $1 \text{ kg m}^{-3} \text{ d}^{-1}$ . The COD removal efficiency was approximately 30%. On a percentage basis, the air-cathode MFCs removed an average of  $52 \pm 19\%$  of the influent COD (Rossi and Logan, 2022).

The HRT is a critical factor influencing COD removal efficiency (Bird et al., 2022). The effect of HRT on COD removal in MFC has been previously reported (Hiegemann et al., 2019; Sharma and Li, 2010; Sobieszuk et al., 2017; Sugioka et al., 2022). Longer HRT leads to longer residence time for organic matter in the anode chamber, providing higher contact time for microorganisms to oxidize the organics and transfer the electrons, resulting in higher COD removal efficiency and increased energy output (Subha et al., 2019; Ye et al., 2020). It is important to highlight that several other factors could influence COD degradation, including the optimal ratio of anode surface area to reactor volume and biofilm structure in the anode (Huang et al., 2022).

In addition, the COD removal may be explained by the external resistance ( $R_{\text{ext}} = 1000 \Omega$ ). The removal of COD can be explained by the impact of external resistance on the rate of electron transfer, metabolic activity, and organic degradation kinetics (Zhang et al., 2011). Lower external resistors improve pollutant removal due to activation and ohmic overpotential reduction. Perazzoli (2018) observed that  $22 \Omega$  external resistor provides a maximum acetate consumption rate of  $293.01 \text{ mg L.h}^{-1}$ . At  $560 \Omega$ , the rate was  $250 \text{ mg L.h}^{-1}$ . Yang et al. (2022) also reported that the average COD removal efficiency decreased from  $85.63 \pm 0.08\%$  to  $82.70 \pm 0.31\%$  as the external resistance changed from 200 to 2000  $\Omega$ . Therefore, changing the external resistance could improve COD removal.

To complete the COD removal and attempt the environmental rules for discharge, several studies have suggested the use of additional technologies further to treat the MFC effluent, such as biofilter (Rossi et al., 2022), anaerobic fluidized bed membrane bioreactor (Ren et al., 2014), and wetland (Lutterbeck et al., 2020).

The CE obtained in HRT 12, 8, and 4 h was 5.44, 2.23, and 1.12%, respectively. The highest CE was observed at an HRT of 12 h, while the CE decreased gradually as the HRT was reduced. This suggests that a large number of substrates may be used for anaerobic biodegradation, but only a small amount of oxidized substrates was available as electron donors for power generation (Subha et al., 2019; Tamilarasan et al., 2017).

There are three key aspects that control CE in an MFC, such as microbial activity; competitiveness for electron donors; and dissolved oxygen concentration in the anode chamber (Cano et al., 2021). CE is reduced when some substrates are used for anaerobic processes like methane production and fermentation rather than for the metabolism of electroactive bacteria (Subha et al., 2019; Zhuang et al., 2012).

### 3.2.2. Nutrient removal

$\text{NH}_4^+$  (ammoniacal nitrogen),  $\text{NO}_3^-$  (nitrate) and TN concentration in raw wastewater and effluent was monitored. The obtained results are presented in Table 3.

The results obtained suggest a low ammonia removal efficiency. The nitrification is considered the main pathway for the transformation of

**Table 3**

Physical-chemical characterization of the raw wastewater and effluent of each strategy during MFC operation.

| Parameter                     |                  | Raw wastewater | Effluent strategy I | Effluent strategy II | Effluent strategy III |
|-------------------------------|------------------|----------------|---------------------|----------------------|-----------------------|
| COD <sub>T</sub>              | mg               | 634.33 ±       | 643.2 ±             | 636.7 ±              | 650.3 ±               |
|                               | L <sup>-1</sup>  | 15.87          | 17.65               | 13.84                | 16.69                 |
| NH <sub>4</sub> <sup>+</sup>  | mg               | 47.18 ±        | 45.26 ±             | 46.03 ±              | 45.89 ±               |
|                               | L <sup>-1</sup>  | 4.18           | 2.81                | 6.05                 | 2.70                  |
| NO <sub>3</sub> <sup>-</sup>  | mg               | 0.05 ± 0.03    | 0.03 ±              | 0.04 ±               | 0.03 ±                |
|                               | L <sup>-1</sup>  |                | 0.01                | 0.01                 | 0.02                  |
| TN                            | mg               | 49.91 ±        | 47.67 ±             | 49.50 ±              | 49.19 ±               |
|                               | L <sup>-1</sup>  | 3.03           | 8.64                | 5.18                 | 1.29                  |
| PO <sub>4</sub> <sup>3-</sup> | mg               | 6.31 ± 0.43    | 6.70 ±              | 6.81 ±               | 6.43 ±                |
|                               | L <sup>-1</sup>  |                | 0.65                | 0.40                 | 0.48                  |
| SO <sub>4</sub> <sup>2-</sup> | mg               | 22.92 ±        | 18.87 ±             | 17.57 ±              | 8.80 ±                |
|                               | L <sup>-1</sup>  | 11.24          | 0.93                | 6.40                 | 2.96                  |
| Cl <sup>-</sup>               | mg               | 101.35 ±       | 147.45 ±            | 143.99 ±             | 144.90 ±              |
|                               | L <sup>-1</sup>  | 10.63          | 9.24                | 3.71                 | 6.27                  |
| Acetate                       | mg               | 143.08 ±       | 88.85 ±             | 89.59 ±              | 82.42 ±               |
|                               | L <sup>-1</sup>  | 10.82          | 4.18                | 9.37                 | 10.70                 |
| Alkalinity                    | mg               | 341.41 ±       | 744.40 ±            | 522.22 ±             | 444.44 ±              |
|                               | L <sup>-1</sup>  | 83.90          | 20.30               | 73.70                | 22.22                 |
| pH                            | -                | 7.45 ± 0.29    | 7.90 ±              | 8.04 ±               | 8.03 ±                |
|                               |                  |                | 0.24                | 0.28                 | 0.21                  |
| Conductivity                  | mS               | 1.43 ± 0.09    | 1.42 ±              | 1.35 ±               | 1.31 ±                |
|                               | cm <sup>-1</sup> |                | 0.06                | 0.07                 | 0.04                  |
| TSS                           | mg               | 20.21 ±        | 27.83 ±             | 13.67 ±              | 17.00 ±               |
|                               | L <sup>-1</sup>  | 12.92          | 16.92               | 9.82                 | 13.11                 |
| DO                            | mg               | 4.08 ± 0.76    | 0.85 ±              | 0.88 ±               | 0.34 ±                |
|                               | L <sup>-1</sup>  |                | 0.42                | 0.17                 | 0.37                  |
| Temperature                   | °C               | 27.40 ±        | 28.16 ±             | 27.65 ±              | 28.40 ±               |
|                               |                  | 1.19           | 0.70                | 0.97                 | 1.52                  |

COD<sub>T</sub> – chemical oxygen demand; TN – total nitrogen; | SS – total suspended solids; TDS – total dissolved solids; DO – dissolved oxygen.

$\text{NH}_4^+$  into  $\text{NO}_3^-$  (Rout et al., 2021). Table 3 demonstrates the presence of DO in MFC effluent due to the cathode contact with atmospheric air. These conditions do not permit nitrification, since it requires an aerobic environment with DO levels above  $1.5 \text{ mg L}^{-1}$  (Nguyen and Babel, 2022).

The low amount of ammonia removal observed could be attributed to volatilization through the air-cathode. The hydroxide ions produced during the ORR at the cathode promote a localized pH increase near the cathode (Rossi et al., 2022; Zhuang et al., 2012). The effluent was collected near to cathode and showed pH values equal to  $7.90 \pm 0.24$ ,  $8.04 \pm 0.28$ , and  $8.03 \pm 0.2$  during strategies I, II and III, respectively. Moreover, according to Motoyama et al. (2021), when the electric potential of the anode is high enough, chloride ions in the wastewater can be oxidized to form chlorine, which is then hydrolyzed to hypochlorous acid. This acid can further react with ammonia, resulting in a reduction in ammonia concentration.

At the same time, the nitrate and acetate show minor concentrations after the MFC treatment (Table 3). This could indicate that the dominant pathway for acetate metabolism in nitrate-reducing cultures was denitrification (Coby et al., 2011). The increase in alkalinity concentration observed in the effluent (Table 3) further supports the idea of the denitrification process, that occurs in anaerobic environment (Nguyen and Babel, 2022). The TN concentration in effluent corroborates with these findings. To elucidate the reason for nitrogen compound removal in the MFCs, it is suggested to analyze microbial communities present in the biofilms on the surface of anode through genetic sequencing.

The orthophosphate ( $\text{PO}_4^{3-}$ ) removal was not identified in this present study. This is due to the fact that biological phosphorus accumulation in excess-sludge biomass is mainly conducted by phosphorus accumulating organisms (PAO), which requires alternating aerobic/anaerobic conditions (Metcalf, 2014). Since the MFC is an anaerobic reactor, PAO are unable to perform their function of degrading the polyphosphate, leading to the release of orthophosphates into the environment. This fact could explain the increase in phosphorous

concentration in the effluent. To date, previous studies have demonstrated the utilization of alternatives electron acceptors in the cathode ( $\text{NO}_3^-$ ,  $\text{PO}_4^{3-}$ ,  $\text{SO}_4^{2-}$ ) aiming the removal or nutrient recovery (Wu et al., 2021; Yang et al., 2019).

In addition, the presence of other electron acceptors in the wastewater, such as sulfate, nitrate, and dissolved oxygen, hinders the complete utilization of COD for electricity production during MFC operation (Su et al., 2018; Subha et al., 2019). For example, the nitrate ions can be converted into molecular nitrogen by denitrification. The COD concentration could be used in this process instead of power generation, lowering the CE, since this process needs a carbon source (Marassi et al., 2020b).

### 3.3. Phytotoxicity assessment

To the best of the authors' knowledge, this study is the first to apply a toxicity tool to evaluate the degree of toxicity for MFC treating municipal wastewater. Compared to the negative control, the GI of the test *L. sativa* seed submitted to the raw wastewater without dilution was 40.33% (Fig. 5). The GI of lettuce seedlings exposed to MFC treated wastewater was higher than that of lettuce seeds exposed to raw wastewater, except for strategy III (Fig. 5). Therefore, it could be assumed that the treatment during strategy I (HRT = 12 h) and strategy II (HRT = 8 h) showed the ability to drop phytotoxic effect present in the raw wastewater.

Root elongation can be more sensitive to chemical compound exposure compared to seed germination, as demonstrated by (Lyu et al., 2018). Based on this, a toxicity test was conducted on all effluent samples using a concentration series of 100%, 75, 50%, and 25% (Table 4). In terms of the  $\text{EC}_{50}$ , root growth inhibition was observed in the raw wastewater (100%) and MFC effluent from strategy III (100%), indicating phytotoxicity for these samples. The wastewater treated by MFC during strategies I and II showed a reduction in toxic potential since it was not possible to calculate the  $\text{EC}_{50}$  for those samples.

The phytotoxic effects produced by wastewater result from a combination of several factors, including the presence of heavy metals, ammonia, high concentrations of ions and volatile organic acids (França Figueiredo et al., 2022; Fuentes et al., 2006). In this study, the observed phytotoxicity could be attributed for zinc, nickel, copper, manganese and iron, utilized in the micronutrient solution for synthetic wastewater production. These micronutrients are essential for plants growth but can be toxic at high concentrations, depending on the medium used (Lyu et al., 2018).

In the present work, the results of phytotoxicity and physicochemical wastewater characterization were in agreement. The toxic effect assessed across GI could be explained by ammonia presence. Fuentes

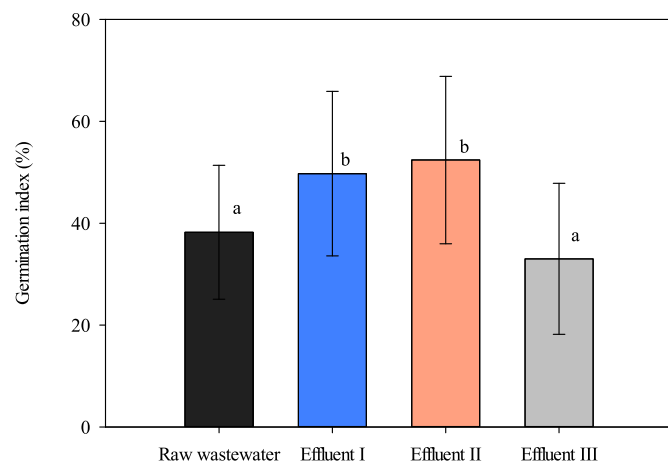


Fig. 5. Germination Index of *L. sativa* seeds for raw wastewater and different treatment strategies.

Table 4

Phytotoxicity effects on *L. sativa* root elongation (cm), expressed as  $\text{EC}_{50}$ .

| Sample         | Tested effluent concentration (%) |             |             |             | $\text{EC}_{50(\%)}$        |
|----------------|-----------------------------------|-------------|-------------|-------------|-----------------------------|
|                | 25                                | 50          | 75          | 100         |                             |
| Raw wastewater | 1.61 ± 0.70                       | 1.59 ± 0.62 | 1.05 ± 0.40 | 0.73 ± 0.25 | <b>87.72</b>                |
| Effluent I     | 2.06 ± 0.63                       | 1.30 ± 0.40 | 1.25 ± 0.42 | 1.20 ± 0.37 | Not calculable <sup>a</sup> |
| Effluent II    | 1.15 ± 0.24                       | 0.97 ± 0.27 | 0.86 ± 0.14 | 0.83 ± 0.27 | Not calculable <sup>a</sup> |
| Effluent III   | 1.21 ± 0.57                       | 1.16 ± 0.51 | 0.92 ± 0.28 | 0.59 ± 0.30 | <b>82.09</b>                |

<sup>a</sup> It was not possible to calculate the  $\text{EC}_{50}$ , because even when exposed to 100% of the sample there was no effect on 50% of the organisms.

et al. (2006) have reported that the presence of ammonia in anaerobic sludges could have a negative influence on seed germination and growth. However, the concentration of  $\text{NH}_4^+$  was found to be lower after the treatment, which could explain the increase in GI observed in strategy I and II. Considering the wastewater treatment, the strategy I showed the best performance, and a significant difference in GI was found. Therefore, it might be suggested that strategy I produced an effluent with lower toxic potential.

However, wastewater treatment does not always lead to a reduction in effluent toxicity and may, in some cases, even increase it (Yu et al., 2019). In this study, strategy III showed the worst performance for wastewater treatment. This result reflects in phytotoxicity removal. This finding could be explained by the synergism effect of various pollutants present in the effluents, which may have contributed to the development of harmful intermediates during the fast treatment under 4 h (França Figueiredo et al., 2022; Gerber et al., 2017).

Our findings are consistent with prior research on the toxicity of MFC effluents, indicating the potential of toxicity reduction (Lutterbeck et al., 2020; Marassi et al., 2020a). The *Lactuca sativa* ecotoxicity assay supports the conclusion that an HRT of 12 h could be considered optimal for this study and could be applied as a complementary method to routine analysis to gather toxicological information.

### 3.4. Implications in the integration of MFC in the wastewater treatment system

The development of this research aimed to mimic the actual conditions of conventional WWTPs. Therefore, continuous mode flow, HRT, and OLR values aligned with this proposal were employed. Generally, researchers employ batch operation in MFC due to the ease of operation. However, several authors show less efficiency in this model due to less time available for biological activity (Bird et al., 2022). Thus, obtaining optimal performance in continuous flow can be considered a challenge in MFC technology.

In addition, scaling up the MFC up to 2 L and increasing the electrode area to 132  $\text{cm}^2$  aims to contribute to applying the technology in practical situations. These values are higher than commonly reported values in the literature (Yu et al., 2021). Marassi et al., (2020a) have operated a MFC with a similar configuration and size in batch mode with dairy effluent, achieving The current density ranged from 210 to 125  $\text{mA m}^{-3}$ , similar to that obtained in this present research. Moreover, the inoculation procedure utilized anaerobic sludge from WWTP, demonstrating the feasibility of MFC for integrating the MFC into the wastewater treatment infrastructure (Ghangrekar and Shinde, 2008).

From this perspective, the MFC could be operated as a primary effluent treatment (He et al., 2019). According to Metcalf (2014), primary effluent treatment typically achieves a COD removal efficiency of 25% to 40%. Further treatment technologies may be necessary to meet environmental regulations, mainly for remaining COD and nutrients.

Therefore, applying MFC for wastewater treatment will change the wastewater and energy sectors, transforming WWTPs from elevated

energy consumers into sustainable energy producers. Future research should enhance the technology's energy generation and storage capabilities before integrating it into WWTPs.

#### 4. Conclusion

The study provides insights about the HRT on the performance of a scaled-up air-cathode MFC operating in continuous flow mode. The results demonstrated that longer HRTs lead to significantly improved MFC performance, including higher power density, coulombic efficiency, and COD removal, as well as reduced effluent toxicity. These findings have important implications for the configuration and operation of MFCs, as they suggest that longer HRTs can enable more efficient and effective wastewater treatment and increased electricity generation. Furthermore, applying toxicity tools is an excellent alternative to improve the monitoring of MFC effluent quality, which can enhance the overall reliability and effectiveness of MFC-based wastewater treatment systems, mainly for WWTPs. Moreover, the MFC effluent characteristics indicated that the assessed MFC could be applied as a first-step treatment unit in a WWTP. Future research should focus on further improving the COD and nutrient removal efficiency of MFCs and exploring new approaches for recovering the electricity produced. Altogether, our study highlights the potential of air-cathode MFCs as a promising technology for sustainable wastewater treatment and energy production.

#### Credit author statement

Ana Carla Sorgato: Conceptualization, Methodology, Formal analysis, Investigation, Data curation, Writing – original draft. Thamires Custódio Jeremias: Investigation, Writing – review & editing. Fernanda Leite Lobo: Writing – review & editing, Supervision. Flávio Rubens Lapolli: Writing – review & editing, Supervision, Project administration, Funding acquisition.

#### Declaration of competing interest

The authors declare the following financial interests/personal relationships which may be considered as potential competing interests: Ana Carla Sorgato reports financial support was provided by Coordination for the Improvement of Higher Education Personnel (CAPES). Thamires Custódio Jeremias reports financial support was provided by Coordination for the Improvement of Higher Education Personnel (CAPES).

#### Data availability

Data will be made available on request.

#### Acknowledgments

The authors are grateful to the Federal University of Santa Catarina (UFSC) for the technical support and the Coordination for the Improvement of Higher Education Personnel (CAPES) for financial support (Finance Code 001).

#### References

Ahn, Y., Logan, B.E., 2010. Effectiveness of domestic wastewater treatment using microbial fuel cells at ambient and mesophilic temperatures. *Bioresour. Technol.* 101, 469–475. <https://doi.org/10.1016/j.biortech.2009.07.039>.  
 APHA, 2005. *Standard Methods for the Examination of Water and Wastewater, twenty-first ed.* American Public Health Association/American Water Works Association/Water Environment Federation, Washington DC.  
 Bird, H., Heidrich, E.S., Leicester, D.D., Theodosiou, P., 2022. Pilot-scale Microbial Fuel Cells (MFCs): a meta-analysis study to inform full-scale design principles for optimum wastewater treatment. *J. Clean. Prod.* 346, 131227. <https://doi.org/10.1016/j.jclepro.2022.131227>.

Brehehy, M., Bowman, K., Farahmand, N., Gomaa, O., Keshavarz, T., Kyazze, G., 2019. Biocatalytic electrode improvement strategies in microbial fuel cell systems. *J. Chem. Technol. Biotechnol.* 94, 2081–2091. <https://doi.org/10.1002/jctb.5916>.  
 Cano, V., Cano, J., Nunes, S.C., Nolasco, M.A., 2021. Electricity generation influenced by nitrogen transformations in a microbial fuel cell: assessment of temperature and external resistance. *Renew. Sustain. Energy Rev.* 139, 110590. <https://doi.org/10.1016/j.rser.2020.110590>.  
 Coby, A.J., Picardal, F., Shelobolina, E., Xu, H., Roden, E.E., 2011. Repeated anaerobic microbial redox cycling of iron. *Appl. Environ. Microbiol.* 77, 6036–6042. [https://doi.org/10.1128/AEM.00276-11/SUPPL\\_FILE/AEM00276\\_11\\_VERSION\\_2\\_SUPPLEMENTAL.DOC](https://doi.org/10.1128/AEM.00276-11/SUPPL_FILE/AEM00276_11_VERSION_2_SUPPLEMENTAL.DOC).  
 Colares, G.S., Dell'Osbel, N., Barbosa, C.V., Lutterbeck, C., Oliveira, G.A., Rodrigues, L. R., Bergmann, C.P., Lopez, D.R., Rodriguez, A.L., Vymazal, J., Machado, E.L., 2021. Floating treatment wetlands integrated with microbial fuel cell for the treatment of urban wastewaters and bioenergy generation. *Sci. Total Environ.* 766, 142474. <https://doi.org/10.1016/j.scitotenv.2020.142474>.  
 Deng, S., Wang, C., Hao Ngo, H., Guo, W., You, N., Tang, H., Yu, H., Tang, L., Han, J., 2023. Comparative review on microbial electrochemical technologies for resource recovery from wastewater towards circular economy and carbon neutrality. *Bioresour. Technol.* 376, 128906. <https://doi.org/10.1016/j.biortech.2023.128906>.  
 Dwivedi, K.A., Huang, S.J., Wang, C.T., Kumar, S., 2022. Fundamental understanding of microbial fuel cell technology: recent development and challenges. *Chemosphere* 288, 132446. <https://doi.org/10.1016/j.chemosphere.2021.132446>.  
 Environmental Canada, 2007. Guidance document on statistical methods for environmental toxicity tests. *Environ. Prot. Ser. EPS 1/RM/46*, 2005 with 2007 Update. 280 p.  
 Fadzli, F.S., Bhawani, S.A., Mohammad, R.E.A., 2021. Microbial fuel cell: recent developments in organic substrate use and bacterial electrode interaction. *J. Chem.* 2021, 1–16. <https://doi.org/10.1155/2021/4570388>.  
 França Figueiredo, F., Karoliny Formicoli de Souza Freitas, T., Gonçalves Dias, G., Cesar Lopes Geraldino, H., Paula Jambers Scandelai, A., Junkes Vilvert, A., Carla Garcia, J., 2022. Textile-effluent treatment using Aloe vera mucilage as a natural coagulant prior to a photo-Fenton reaction. *J. Photochem. Photobiol. Chem.* 429, 113948. <https://doi.org/10.1016/j.jphotochem.2022.113948>.  
 Fuentes, A., Lloréns, M., Sáez, J., Aguilar, M.I., Pérez-Marín, A.B., Ortuño, J.F., Meseguer, V.F., 2006. Ecotoxicity, phytotoxicity and extractability of heavy metals from different stabilised sewage sludges. *Environ. Pollut.* 143, 355–360. <https://doi.org/10.1016/j.envpol.2005.11.035>.  
 Gerber, M.D., Lucia, T., Correa, L., Neto, J.E.P., Correa, É.K., 2017. Phytotoxicity of effluents from swine slaughterhouses using lettuce and cucumber seeds as bioindicators. *Sci. Total Environ.* 592, 86–90. <https://doi.org/10.1016/j.scitotenv.2017.03.075>.  
 Ghangrekar, M.M., Shinde, V.B., 2008. Simultaneous sewage treatment and electricity generation in membrane-less microbial fuel cell. *Water Sci. Technol.* 58, 37–43. <https://doi.org/10.2166/wst.2008.339>.  
 Haavisto, J.M., Kokko, M.E., Lay, C.H., Puhakka, J.A., 2017. Effect of hydraulic retention time on continuous electricity production from xylose in up-flow microbial fuel cell. *Int. J. Hydrogen Energy* 42, 27494–27501. <https://doi.org/10.1016/j.ijhydene.2017.05.068>.  
 He, W., Dong, Y., Li, C., Han, X., Liu, J., Feng, Y., 2019. Field tests of cubic-meter scale microbial electrochemical system in a municipal wastewater treatment plant. *Water Res.* 155, 372–380. <https://doi.org/10.1016/j.watres.2019.01.062>.  
 Hiegemann, H., Littfinski, T., Krimmler, S., Lübben, M., Klein, D., Schmelz, K.G., Ooms, K., Pant, D., Wichern, M., 2019. Performance and inorganic fouling of a submersible 255 L prototype microbial fuel cell module during continuous long-term operation with real municipal wastewater under practical conditions. *Bioresour. Technol.* 294, 122227. <https://doi.org/10.1016/j.biortech.2019.122227>.  
 Huang, S.-J., Dwivedi, K.A., Kumar, S., Wang, C.-T., 2022. Multiwall carbon nanotubes-coated graphite-felt anode for efficient removal of ciprofloxacin from domestic wastewater in dual-chambered microbial fuel cells. *J. Environ. Eng.* 148, 04022022. [https://doi.org/10.1061/\(ASCE\)EE.1943-7870.0001991](https://doi.org/10.1061/(ASCE)EE.1943-7870.0001991).  
 Jeremias, T.C., 2019. Estudo do potencial de biossorbentes de baixo custo para remediação de águas fluviais contaminadas com drenagem ácida mineral (DAM) visando o seu uso secundário não potável. Universidade Federal de Santa Catarina.  
 Kim, K.Y., Yang, W., Logan, B.E., 2015. Impact of electrode configurations on retention time and domestic wastewater treatment efficiency using microbial fuel cells. *Water Res.* 80, 41–46. <https://doi.org/10.1016/j.watres.2015.05.021>.  
 Li, W.W., Yu, H.Q., Rittmann, B.E., 2015. Chemistry: reuse water pollutants. *Nat.* 528, 29–31. <https://doi.org/10.1038/528029a>, 2015.  
 Liu, H., Cheng, S., Huang, L., Logan, B.E., 2008. Scale-up of membrane-free single-chamber microbial fuel cells. *J. Power Sources* 179, 274–279. <https://doi.org/10.1016/j.jpowsour.2007.12.120>.  
 Lobo, F.L., Wang, X., Ren, Z.J., 2017. Energy harvesting influences electrochemical performance of microbial fuel cells. *J. Power Sources* 356, 356–364. <https://doi.org/10.1016/j.jpowsour.2017.03.067>.  
 Logan, B.E., Hamelers, B., Rozendal, R., Schröder, U., Keller, J., Freguía, S., Aelterman, P., Verstraete, W., Rabaey, K., 2006. Microbial fuel cells: methodology and technology. *Environ. Sci. Technol.* 40, 5181–5192. <https://doi.org/10.1021/es0605016>.  
 Logan, B.E., Rossi, R., Ragab, A., Saikaly, P.E., 2019. Electroactive microorganisms in bioelectrochemical systems. *Nat. Rev. Microbiol.* 17, 307–319. <https://doi.org/10.1038/s41579-019-0173-x>.  
 Luo, J., Tian, W., Jin, H., Yang, J., Li, J., Wang, Y., Shen, W., Ren, Y., Zhou, M., 2023. Recent advances in microbial fuel cells: a review on the identification technology,

- molecular tool and improvement strategy of electricigens. *Curr. Opin. Electrochem.* 37, 101187 <https://doi.org/10.1016/j.coelec.2022.101187>.
- Lutterbeck, C.A., Machado, E.L., Sanchez-Barrios, A., Silveira, E.O., Layton, D., Rieger, A., Lobo, E.A., 2020. Toxicity evaluation of hospital laundry wastewaters treated by microbial fuel cells and constructed wetlands. *Sci. Total Environ.* 729 <https://doi.org/10.1016/j.scitotenv.2020.138816>.
- Lyu, J., Park, J., Kumar Pandey, L., Choi, S., Lee, H., De Saeger, J., Depuydt, S., Han, T., 2018. Testing the toxicity of metals, phenol, effluents, and receiving waters by root elongation in *Lactuca sativa* L. *Ecotoxicol. Environ. Saf.* 149, 225–232. <https://doi.org/10.1016/j.ecoenv.2017.11.006>.
- Marassi, R.J., Queiroz, L.G., Silva, D.C.V.R., dos Santos, F.S., Silva, G.C., de Paiva, T.C.B., 2020a. Long-term performance and acute toxicity assessment of scaled-up air-cathode microbial fuel cell fed by dairy wastewater. *Bioproc. Biosyst. Eng.* 43, 1561–1571. <https://doi.org/10.1007/s00449-020-02348-y>.
- Marassi, R.J., Queiroz, L.G., Silva, D.C.V.R., Silva, F.T., da, Silva, G.C., Paiva, T.C.B.d., 2020b. Performance and toxicity assessment of an up-flow tubular microbial fuel cell during long-term operation with high-strength dairy wastewater. *J. Clean. Prod.* 259, 120882 <https://doi.org/10.1016/j.jclepro.2020.120882>.
- Metcalfe, Eddy, 2014. *Wastewater Engineering - Treatment and Resource Recovery*, 5<sup>th</sup> edition. McGraw-Hi, Boston.
- Motoyama, A., Ichihashi, O., Hirooka, K., 2021. Is ammonia volatilization a main mechanism of ammonia loss in single-chamber microbial fuel cells? *Int. J. Environ. Sci. Technol.* 18, 781–786. <https://doi.org/10.1007/S13762-020-02895-7/FIGURES/6>.
- Munoz-Cupa, C., Hu, Y., Xu, C., Bassi, A., 2021. An overview of microbial fuel cell usage in wastewater treatment, resource recovery and energy production. *Sci. Total Environ.* 754, 142429 <https://doi.org/10.1016/j.scitotenv.2020.142429>.
- Nguyen, H.D., Babel, S., 2022. Insights on microbial fuel cells for sustainable biological nitrogen removal from wastewater: a review. *Environ. Res.* 204, 112095 <https://doi.org/10.1016/j.envres.2021.112095>.
- Opoku, P.A., Jingyu, H., Yi, L., Guang, L., Norgbey, E., 2022. Scaled-up multi-anode shared cathode microbial fuel cell for simultaneous treatment of multiple real wastewaters and power generation. *Chemosphere* 299, 134401. <https://doi.org/10.1016/j.chemosphere.2022.134401>.
- Penteado, E.D., Fernandez-Marchante, C.M., Zaiat, M., Cañizares, P., Gonzalez, E.R., Rodrigo, M.A., 2016. Influence of sludge age on the performance of MFC treating winery wastewater. *Chemosphere* 151, 163–170. <https://doi.org/10.1016/j.chemosphere.2016.01.030>.
- Perazzoli, S., 2018. *Célula Microbiana de Dessalinização com Biocátodo Anódico para Simultânea remoção de carbono e nitrogênio, geração de bioeletricidade e dessalinização*. Universidade Federal de Santa Catarina, Florianópolis.
- Ren, L., Ahn, Y., Logan, B.E., 2014. A two-stage microbial fuel cell and anaerobic fluidized bed membrane bioreactor (MFC-AFMBR) system for effective domestic wastewater treatment. *Environ. Sci. Technol.* 48, 4199–4206. <https://doi.org/10.1021/es500737m>.
- Rossi, R., Hur, A.Y., Page, M.A., Thomas, A.O.B., Butkiewicz, J.J., Jones, D.W., Baek, G., Saikaly, P.E., Crokek, D.M., Logan, B.E., 2022. Pilot scale microbial fuel cells using air cathodes for producing electricity while treating wastewater. *Water Res.* 215, 118208 <https://doi.org/10.1016/j.watres.2022.118208>.
- Rossi, R., Logan, B.E., 2022. Impact of reactor configuration on pilot-scale microbial fuel cell performance. *Water Res.* 225, 119179 <https://doi.org/10.1016/j.watres.2022.119179>.
- Rossi, R., Yang, W., Zikmund, E., Pant, D., Logan, B.E., 2018. In situ biofilm removal from air cathodes in microbial fuel cells treating domestic wastewater. *Bioresour. Technol.* 265, 200–206. <https://doi.org/10.1016/j.biortech.2018.06.008>.
- Rout, P.R., Shahid, M.K., Dash, R.R., Bhunia, P., Liu, D., Varjani, S., Zhang, T.C., Surampalli, R.Y., 2021. Nutrient removal from domestic wastewater: a comprehensive review on conventional and advanced technologies. *J. Environ. Manag.* 296, 113246 <https://doi.org/10.1016/j.jenvman.2021.113246>.
- Sharma, Y., Li, B., 2010. Optimizing energy harvest in wastewater treatment by combining anaerobic hydrogen producing biofermentor (HPB) and microbial fuel cell (MFC). *Int. J. Hydrogen Energy* 35, 3789–3797. <https://doi.org/10.1016/j.ijhydene.2010.01.042>.
- Sobieszuk, P., Zamojska-Jaroszewicz, A., Makowski, Ł., 2017. Influence of the operational parameters on bioelectricity generation in continuous microbial fuel cell, experimental and computational fluid dynamics modelling. *J. Power Sources* 371, 178–187. <https://doi.org/10.1016/j.jpowsour.2017.10.032>.
- Sobrero, M.C., Ronco, A., 2004. *Ensayos de toxicidad aguda con semillas de lechuga Lactuca sativa L.*
- Sorgato, A.C., Jeremias, T.C., Lobo, F.L., Lapolli, F.R., 2022. Bioelectricity generation in microbial fuel cell by a membrane electrode assemble: startup assessment. In: *International Conference on Innovations in Energy Engineering & Cleaner Production IEE CP*, p. 1.
- Souza, E., Follmann, H.V.D.M., Dalri-Cecato, L., Battistelli, A.A., Lobo-Recio, M.A., Belli, T.J., Lapolli, F.R., 2020. Membrane fouling suppression using intermittent electric current with low exposure time in a sequencing batch membrane bioreactor. *J. Environ. Chem. Eng.* 8, 104018 <https://doi.org/10.1016/j.jece.2020.104018>.
- Su, S., gang, Cheng, H. yi, Zhu, T., ting, Wang, cheng, H., Wang, A., jie, 2018. Kinetic competition between microbial anode respiration and nitrate respiration in a bioelectrochemical system. *Bioelectrochemistry* 123, 241–247. <https://doi.org/10.1016/j.bioelechem.2018.06.001>.
- Subha, C., Kavitha, S., Abisheka, S., Tamilarasan, K., Arulazhagan, P., Rajesh Banu, J., 2019. Bioelectricity generation and effect studies from organic rich chocolate waste wastewater using continuous upflow anaerobic microbial fuel cell. *Fuel* 251, 224–232. <https://doi.org/10.1016/j.fuel.2019.04.052>.
- Sugioka, M., Yoshida, N., Yamane, T., Kakihana, Y., Higa, M., Matsumura, T., Sakoda, M., Iida, K., 2022. Long-term evaluation of an air-cathode microbial fuel cell with an anion exchange membrane in a 226L wastewater treatment reactor. *Environ. Res.* 205, 112416 <https://doi.org/10.1016/j.envres.2021.112416>.
- Tamilarasan, K., Banu, J.R., Jayashree, C., Yagalakshmi, K.N., Gokulakrishnan, K., 2017. Effect of organic loading rate on electricity generating potential of upflow anaerobic microbial fuel cell treating surgical cotton industry wastewater. *J. Environ. Chem. Eng.* 5, 1021–1026. <https://doi.org/10.1016/j.jece.2017.01.025>.
- Walter, X.A., Madrid, E., Gajda, I., Greenman, J., Ieropoulos, I., 2022. Microbial fuel cell scale-up options: performance evaluation of membrane (c-MFC) and membrane-less (s-MFC) systems under different feeding regimes. *J. Power Sources* 520, 230875. <https://doi.org/10.1016/j.jpowsour.2021.230875>.
- Wu, M., Liu, J., Gao, B., Sillanpää, M., 2021. Phosphate substances transformation and vivianite formation in P-Fe containing sludge during the transition process of aerobic and anaerobic conditions. *Bioresour. Technol.* 319 <https://doi.org/10.1016/j.biortech.2020.124259>.
- Yang, H., Chen, J., Yu, L., Li, W., Huang, X., Qin, Q., Zhu, S., 2022. Performance optimization and microbial community evaluation for domestic wastewater treatment in a constructed wetland-microbial fuel cell. *Environ. Res.* 212, 113249 <https://doi.org/10.1016/j.envres.2022.113249>.
- Yang, N., Zhan, G., Li, D., Wang, X., He, X., Liu, H., 2019. Complete nitrogen removal and electricity production in Thauera-dominated air-cathode single chambered microbial fuel cell. *Chem. Eng. J.* 356, 506–515. <https://doi.org/10.1016/j.cej.2018.08.161>.
- Yang, W., Wang, X., Rossi, R., Logan, B.E., 2020. Low-cost Fe–N–C catalyst derived from Fe (III)-chitosan hydrogel to enhance power production in microbial fuel cells. *Chem. Eng. J.* 380, 122522 <https://doi.org/10.1016/j.cej.2019.122522>.
- Ye, Y., Ngo, H.H., Guo, W., Chang, S.W., Nguyen, D.D., Zhang, X., Zhang, S., Luo, G., Liu, Y., 2020. Impacts of hydraulic retention time on a continuous flow mode dual-chamber microbial fuel cell for recovering nutrients from municipal wastewater. *Sci. Total Environ.* 734, 139220 <https://doi.org/10.1016/j.scitotenv.2020.139220>.
- Yu, J., Park, Y., Widyarningsih, E., Kim, S., Kim, Y., Lee, T., 2021. Microbial fuel cells: devices for real wastewater treatment, rather than electricity production. *Sci. Total Environ.* 775, 145904 <https://doi.org/10.1016/j.scitotenv.2021.145904>.
- Yu, Y., Wu, B., Jiang, L., Zhang, X.X., Ren, H.Q., Li, M., 2019. Comparative analysis of toxicity reduction of wastewater in twelve industrial park wastewater treatment plants based on battery of toxicity assays. *Sci. Rep.* 9, 1–10. <https://doi.org/10.1038/s41598-019-40154-z>, 2019.
- Zhang, L., Zhu, X., Li, J., Liao, Q., Ye, D., 2011. Biofilm formation and electricity generation of a microbial fuel cell started up under different external resistances. *J. Power Sources* 196, 6029–6035. <https://doi.org/10.1016/j.jpowsour.2011.04.013>.
- Zhao, S., Yun, H., Khan, A., Salama, E.S., Redina, M.M., Liu, P., Li, X., 2022. Two-stage microbial fuel cell (MFC) and membrane bioreactor (MBR) system for enhancing wastewater treatment and resource recovery based on MFC as a biosensor. *Environ. Res.* 204, 112089 <https://doi.org/10.1016/j.envres.2021.112089>.
- Zhuang, L., Zheng, Y., Zhou, S., Yuan, Y., Yuan, H., Chen, Y., 2012. Scalable microbial fuel cell (MFC) stack for continuous real wastewater treatment. *Bioresour. Technol.* 106, 82–88. <https://doi.org/10.1016/j.biortech.2011.11.019>.